Dark Current Degradation of Near Infrared Avalanche Photodiodes From Proton Irradiation

Heidi N. Becker and Allan H. Johnston, *Fellow, IEEE*

***Abstract*—InGaAs and Ge avalanche photodiodes (APDs) are examined for the effects of 63-MeV protons on dark current. Dark current increases were large and similar to prior results for silicon APDs, despite the smaller size of InGaAs and Ge devices. Bulk dark current increases from displacement damage in the depletion regions appeared to be the dominant contributor to overall dark current degradation. Differences in displacement damage factors are discussed as they relate to structural and material differences between devices.**

***Index Terms*—Avalanche photodiodes, dark current, displacement damage, Ge, InGaAs, protons.**

I. Introduction

THERE continues to be a strong interest in the use of avalanche photodiodes (APDs) as space-borne optical communications data receivers. APDs are an attractive receiver choice for photon starved communications applications, because their internal gain mechanism can improve signal to noise ratio. The appropriate APD for a particular application offers an advantageous combination of several factors, including high quantum efficiency, high frequency response, low noise, and high gain [1]. Radiation-induced changes in dark current are important to quantify, because dark current changes are an important component of such figures of merit as signal to noise ratio and noise equivalent power (NEP). The total spectral noise current of an unilluminated APD is given by

$$i_n = \left[2q(I_{\rm ds} + I_{\rm db}M^2F)B\right]^{\frac{1}{2}} \quad (1)$$

where $I_{\rm ds}$ is the unmultiplied surface dark current, $I_{\rm db}$ is the gain-multiplied bulk dark current, M is the gain, F is the excess noise factor, and B is the noise bandwidth [2]. Total dark current (I_d) is related to the parameters in (1) by

$$I_d = I_{\rm ds} + MI_{\rm db}. \quad (2)$$

Ultimately, increases in detector dark current (and, therefore, noise) increase the probability of bit-error rate (BER) in digital communications, the exact degree of which is dependent on the encoding scheme in question [3], [4].

Manuscript received July 20, 2004; revised September 10, 2004. The research in this paper was carried out at the Jet Propulsion Laboratory, California Institute of Technology, under contract with the National Aeronautics and Space Administration (NASA), under the NASA Electronic Parts and Packaging Program, Code Q.

The authors are with the Jet Propulsion Laboratory, California Institute of Technology, Pasadena, CA 91109 USA (e-mail: Heidi.N.Becker@jpl.nasa.gov; Allan.H.Johnston@jpl.nasa.gov).

Digital Object Identifier 10.1109/TNS.2004.839165

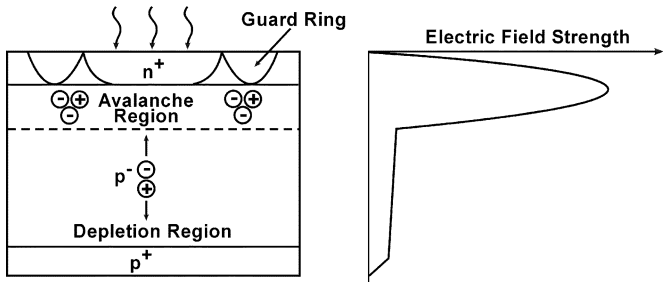

Fig. 1. Avalanche photodiode structure.

An optical communications receiver must also be appropriate for the laser wavelength being used. In previous work we presented gamma and 51-MeV proton results for several silicon APD structures, including a near IR-enhanced Si APD appropriate for 1064 nm systems [5]. Silicon detectors have a long-wavelength responsivity cutoff at 1.1 μm, which corresponds to the wavelength of its bandgap. Therefore, detectors made from materials with higher absorption coefficients at long wavelengths are necessary for near infrared applications [6]. The near infrared is the preferred wavelength regime for deep space optical communications. This paper discusses proton and gamma radiation degradation in Ge and InGaAs APDs suitable for wavelengths of 1300 and 1550 nm.

Fig. 1 shows a basic APD structure. APDs use a reverse bias applied to a p–n junction. They operate in a fully depleted mode; the reverse bias creates a depletion region in the diode that extends from the junction through the absorption region where photons are absorbed. Absorbed photons create electron-hole pairs in the depletion region. Carriers are swept via drift toward a very high field region near the junction called the avalanche (multiplication) region. Here, carriers create additional e–h pairs through impact ionization, starting the chain reaction of avalanche multiplication (the internal gain mechanism of APDs).

II. Experimental Procedure

Three APDs were selected for the study: two InGaAs APDs (the G8931-03 from Hamamatsu, and the C30645E from Perkin Elmer), and a germanium APD from Judson (J16A-18A-R100U). Key characteristics of the three devices are listed in Table I.

All are high-speed APDs, with cutoff frequencies (the frequency at which the output signal power is down by 3 dB) between 1 and 2 GHz. The quantum efficiency of all three devices is high at 1300 nm, and the InGaAs structures have particularly low dark current at a typical gain (M) of 10, making them good

TABLE I
NEAR INFRARED AVALANCHE PHOTODIODES IN THE STUDY

APD Structure	Active Area Diameter	Cutoff Frequency	QE @ 1300nm	Dark Current (nA)
Hamamatsu ***InGaAs***	30 microns	2 GHz	0.7	~ 6 (M=10)
PerkinElmer ***InGaAs***	80 microns	1 GHz	0.85	~ 1.5 (M=10)
Judson ***Ge***	100 microns	1.5 GHz	0.7	~300 (M=3)

candidates for photon-starved applications in that wavelength regime.

Four samples of each InGaAs APD structure were irradiated at Crocker Nuclear Laboratory, UC Davis, using 63-MeV protons to a fluence of 2×10^{12} p/cm^2. The devices were irradiated and characterized for changes in total dark current (I_d) (leakage current measured at operational voltages under unilluminated conditions), under a constant reverse bias. The voltage was that required for a pre-irradiation gain of approximately 10, and was approximately 0.95 $V_{\rm BR}$ (breakdown voltage) for the Hamamatsu APD and 0.89 $V_{\rm BR}$ for the Perkin Elmer APD. The mean values were 68.5 V and 46.8 V, respectively. The only exception was that one of the four Perkin Elmer samples was irradiated unbiased and characterized at 0.89 $V_{\rm BR}$; no significant difference in post-irradiation behavior was observed compared to the biased test samples. One additional sample of each InGaAs structure was irradiated under bias at the Jet Propulsion Laboratory's Cobalt-60 facility to a cumulative dose of 269 krad(Si) [1.04 Mrad(InGaAs)] to compare proton and gamma radiation effects.

Three samples of the Ge APD were irradiated to 2×10^{12} p/cm^2 at UC Davis. During testing it was determined that similar changes in dark current occurred in biased and unbiased samples. Therefore, only one of the three Judson devices was irradiated under bias, using a voltage that was approximately 0.9 $V_{\rm BR}$ (mean value of 30.9 V); this corresponded to a pre-irradiation gain of approximately 3. All three devices were characterized at 0.9 $V_{\rm BR}$. An additional sample was irradiated under bias using Cobalt-60 gamma radiation to a cumulative dose of 269 krad(Si) [1.01 Mrad(Ge)].

All irradiations were conducted at room temperature. Pre- and post-irradiation characterization was done at 25°C using a thermoelectric cooler (TEC). The temperature of the TEC modules was stable to within ±0.1°C. Characterizations were completed within five minutes after each irradiation to minimize annealing affects, although, in practice, measurements were very stable once the devices reached thermal equilibrium at 25°C.

III. EXPERIMENTAL RESULTS

A. Dark Current Degradation

All three near infrared APDs showed significant dark current degradation following irradiation with 63-MeV protons. Changes in dark current (ΔI_d) were linear with fluence for all three devices, but noticeable differences in damage rates were observed. Increases in dark current, compared to pre-irradiation values (I_{do}), ranged from over an order of magnitude in the Ge APD, to four orders of magnitude in the Perkin Elmer InGaAs APD (by 2×10^{12} p/cm^2). Fig. 2 shows mean changes in dark current, as a function of fluence, for each APD. The error bars in Fig. 2 represent the standard deviation from the mean values.

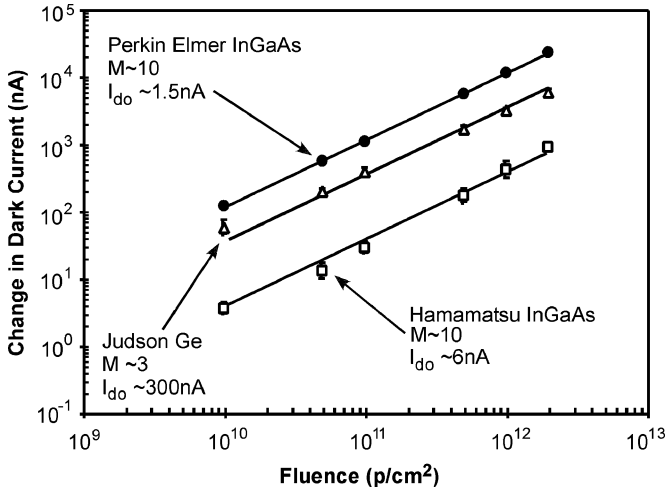

Fig. 2. Mean changes in dark current in InGaAs and Ge APDs following exposure to 63-MeV protons.

The Hamamatsu InGaAs APDs had an average pre-irradiation dark current (I_{do}) of 5.6 nA (at $\mathrm{M} = 10$). At the final cumulative fluence of 2×10^{12} p/cm^2, the APD dark current increased to a mean value of nearly 1 μA (an increase of over two orders of magnitude). Changes in dark current increased linearly with fluence at a rate of approximately 4.5×10^{-10} nA•cm^2/proton. Very little annealing was observed following irradiation. After one month of unbiased annealing at room temperature, the average reduction in dark current was only 80 nA (approximately 8 %).

Although not plotted in Fig. 2, electrical short type failures were observed during post-irradiation characterization of two of our Hamamatsu samples at the higher fluence levels. However, we do not believe that these failures were radiation induced, because there was no evidence of this vulnerability in the other samples, and irradiation was subsequently carried out to 5×10^{12} p/cm^2 on one sample, with no failure. Since no failures were observed in the Perkin Elmer InGaAs or Ge structures, we are confident that the failures were not the result of an instrumentation or test methodology problem. It is most likely that these failures were due to a handling issue during testing.

The Perkin Elmer InGaAs APD showed the highest rate of dark current degradation, at approximately 1.2×10^{-8} nA • cm^2/proton. This rate is 26 times higher than that observed in the Hamamatsu InGaAs APD. The average I_{do} of the Perkin Elmer APD was 1.5 nA (at $M = 10$). This value increased to over 23,000 nA by 2×10^{12} p/cm^2—a 4 order of magnitude increase. The Perkin Elmer APD experienced larger recovery during unbiased annealing at room temperature than the Hamamatsu APD. Dark current values decreased by 10 % within several hours, and by 18 % by the eighth day after irradiation.

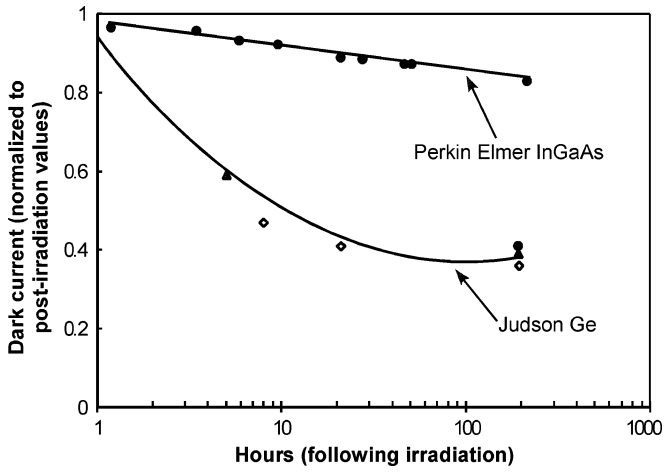

Fig. 3. Dark current reductions during unbiased room temperature annealing of the Ge and Perkin Elmer InGaAs APDs.

TABLE II
NEAR INFRARED APD DAMAGE FACTORS

APD Structure	Damage Factor ($\Delta I_d/\Phi$)
Hamamatsu ***InGaAs***	4.5 x 10^{-10} nA cm^2/p
PerkinElmer ***InGaAs***	1.2 x 10^{-8} nA cm^2/p
Judson ***Ge***	6.0 x 10^{-9} nA cm^2/p

The Ge APDs had a pre-irradiation dark current of 299 nA (at $M = 3$). The damage factor was 6.0×10^{-9} nA $\bullet$ cm^2/proton for this device. The mean value at 2×10^{12} p/cm^2 was approximately 6 μA, over an order of magnitude above the pre-irradiation value. Unlike the InGaAs APDs, this device showed quite significant annealing while unbiased at room temperature, showing a 50% reduction in dark current after several hours. Fig. 3 compares the annealing behavior of the Perkin Elmer InGaAs APD and the Ge APD. It has been noted previously that defect reordering (annealing) is dependent, among other factors, upon material type, impurity type and concentration [7]. It is likely that the material differences in the InGaAs and Ge APDs are responsible for the differences in the observed annealing trends.

Table II summarizes the damage factors for the three APDs in this study.

B. Contribution of Ionization Damage

Previous work with various Si APDs [5] showed that proton-induced increases in dark current were primarily due to displacement damage in the depletion region bulk material. However, ionization damage was shown to cause increased surface dark currents in some devices, depending on the structure. This was attributed to charge trapping in the oxide between guard rings that caused surface currents to flow. In order to determine the extent to which our 63-MeV proton results for InGaAs and Ge APDs are due to displacement damage, Co-60 gamma testing was performed in order to determine if ionization damage (and possible increased surface dark current) was a significant contributor to the overall observed dark current increases. Co-60 gamma radiation causes ionization damage, and only a very small amount of displacement damage compared to protons. It is therefore a good way to identify and isolate displacement damage vs. ionization effects that have been observed with protons. Figs. 4–6 compare 63-MeV proton and Co-60 gamma results for our three APDs.

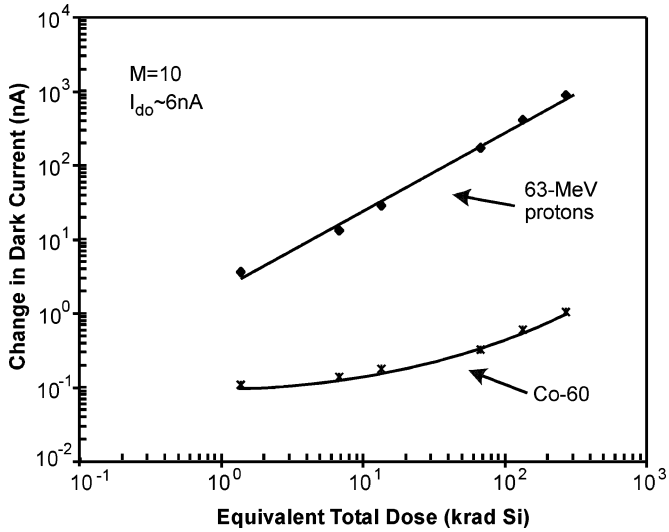

Fig. 4. Comparison of 63-MeV proton and Co-60 results for the Hamamatsu InGaAs APD.

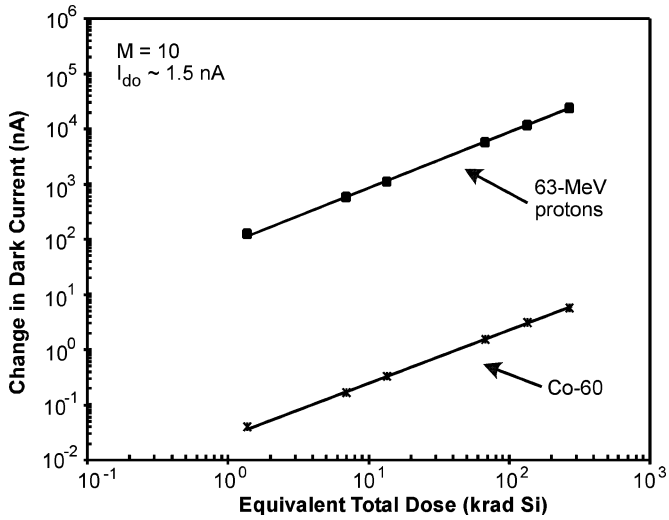

Fig. 5. Comparison of 63-MeV proton and Co-60 results for the Perkin Elmer InGaAs APD.

When comparing 63-MeV proton and Co-60 damage, we expect that the displacement damage ratio will be related to non-ionizing energy loss (NIEL), and that the displacement damage due to proton and gamma radiation will be linear with respect to fluence [8], [9]. As can be seen from Fig. 4 and Fig. 6, there is a nonlinearity to the Co-60 data that indicates a total ionizing dose (TID) effect may be influencing the dark current changes in the Hamamatsu InGaAs and Ge APDs. For the Hamamatsu APD, this effect appears to saturate below 100 krad(Si)(equivalent)

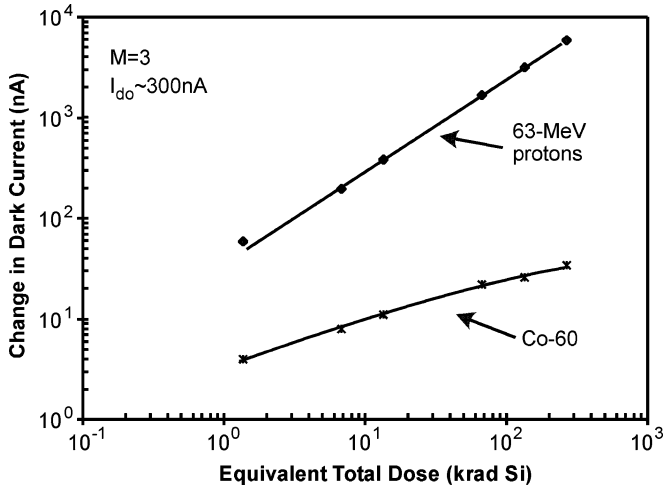

Fig. 6. Comparison of 63-MeV proton and Co-60 results for the Judson Ge APD.

and may be contributing to the slight departure from linearity of the InGaAs proton data at 1 krad(Si)(equivalent). *Nevertheless, TID appears to be responsible for only a very small fraction of the total increases in dark current in all three APD technologies*.

IV. Analysis and Discussion

A. Carrier Generation in Depletion Region Bulk Material

The linearity of the damage in these APDs, and the absence of significant ionization damage, indicates that displacement damage in the APD bulk material is the dominant mechanism affecting dark current degradation. The increases in dark current compared to pre-irradiation values are large and vary significantly among the three studied APDs. In comparing the proton-induced dark current degradation of these near infrared APDs, it is important to note that displacement damage-induced dark current increases in fully depleted silicon detectors have been attributed to the introduction of carrier generation centers in the depletion regions. Such dark current increases have also been found to be directly proportional to the *volume* of the depletion region [5], [10]. Furthermore, in the case of APDs, carriers generated in the depletion region are eventually multiplied via the internal APD avalanche mechanism, so bulk dark current increases for APDs are also gain multiplied.

It is also important to take the material properties of the detector into account when evaluating depletion region damage. For silicon detectors, changes in dark current per unit depletion region volume have been expressed as

$$\frac{\Delta I_d}{V} = \frac{q n_i \phi}{2K_{gn}} \tag{3}$$

where V is the depletion region volume, n_i is the intrinsic carrier density for the detector in question, ϕ is the fluence, and K_{gn} is the damage coefficient for the material type in the depletion region [5], [10]. Analysis of the depletion region volumes *and materials* is necessary in order to evaluate our results.

B. APD Depletion Region Volumes

When APDs are operated for $M > 1$, their depletion regions contain the high field multiplication region and the deeper absorption region where photons are collected. For Ge APDs, the multiplication and absorption regions are both fabricated from Ge, while InGaAs APDs like the ones in this study use separate absorption and multiplication regions where the multiplication region is made from InP, and the active absorption region is made from InGaAs. Fig. 7 shows an InGaAs APD structure similar to the ones in our study.

In order to achieve very high quantum efficiency, the thicknesses of photodiode absorption regions are on the order of $1/\alpha$, where α is the optical absorption coefficient. However, in order to minimize transit time effects and maximize frequency response, absorption regions are kept as narrow as possible without sacrificing too much quantum efficiency [6], [11]. InGaAs APD depletion region thicknesses from 2.5 to 7 μm are common [11], [12], and high speed Ge APDs have depletion regions ranging from several microns to over 100 μm, depending on the wavelength for which they are being optimized [6].

The exact structures of the APDs in this study involve proprietary information. However, in order learn how differences in depletion region volumes could be influencing our results, focused ion beam (FIB) etching and scanning electron microscopy (SEM) analysis was performed to learn about the depletion region thicknesses. For all three APD structures FIB etching was performed to a depth of 15 μm from the surface of the active area. Electron dispersive spectroscopy (EDS) during SEM analysis of our samples allowed us to determine the elemental composition at different depths. In this way, we were able to determine the thicknesses of the InGaAs absorption regions in the Hamamatsu and Perkin Elmer APDs, and use our knowledge of the active area diameters to determine the absorption region volumes (2,650 μm^3 and 11,700 μm^3, respectively). We were also able to identify guard structures in all three APDs.

The Ge APD is not a heterostructure like the InGaAs APDs, so the EDS technique could not be used to learn about the absorption region thickness of this structure. However, information about the device's spectral response allows us to make reasonable assumptions. Although optimized for high speed at 1300 nm, the responsivity of the Ge APD at 1550 nm is about 0.9 A/W. This suggests that the active absorption depth (spanning the depletion region and deeper material where carriers are transported via diffusion) may be close to $1/\alpha$, which for Ge at 1550 nm is around 40 μm. This would make the active collection volume of the Ge APD around 314,000 μm^3.

C. Analysis of Near Infrared APD Results

1) Germanium: Using (1) while taking our approximate knowledge of the material properties of the Ge APD into account [6], and correcting for the operational APD gain, we have reasonable agreement with our results for Si APDs [5]. This allows us to be confident that the dominant mechanism responsible for the dark current degradation in the Ge APD is the introduction of carrier generation centers in the bulk material.

2) InGaAs: Last year, results from 18-MeV oxygen ion irradiation of an InGaAs APD were presented by Laird *et al.* [13]. Although the focus of the study was the single event transient (SET) response of a 2.5-GHz, 50-μm diameter APD, brief analysis of dark current increases as a function of low fluence were

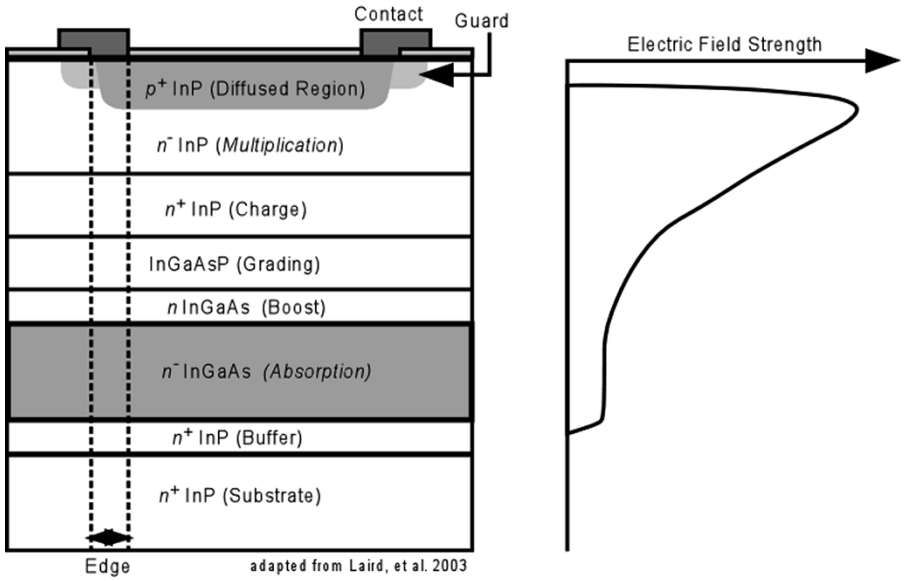

Fig. 7. Schematic of a separate absorption and multiplication InGaAs APD.

presented. The dark I–V characteristics of the APD were examined for voltages from 0 to 50 V after various fluence levels. The group had also experimentally associated bias regimes with specific areas within the APD structure by using CV measurements and transient ion beam-induced current (TIBIC). Their results showed that damage in the InGaAs absorption layer bulk material was the major contributor to dark current increases (the depth of this layer was also presented). Although also present, similar damage in the InP multiplication layer was found to be much less significant.

We compared the damage factor $(\Delta I_d/\phi)$ of Laird *et al.* to those for the InGaAs APDs in our study by correcting for operational gain, normalizing with respect to volume, and using NIEL [9], [14] to correct for the differences in particle type between the Laird *et al.* study and our own. We have very good agreement, indicating that carrier generation in the InGaAs layer is responsible for the dark current degradation we observed in our InGaAs APDs.

What is interesting is that even after normalizing with respect to volume, the damage factor for the Perkin Elmer APD is nearly six times that of the Hamamatsu APD. Our work with Si APDs revealed situations where the presence of ionization damage caused additional surface leakage current, which caused there to be a ratio between the volume-corrected damage factors of different structures. As shown above, ionization does not appear to be a factor with our InGaAs structures. Additionally, unlike the damage we have observed in the present study, the ionization damage we observed in Si APDs was almost exponential, not linear.

D. Carrier Removal Concerns

Carrier removal in the InP multiplication layer or guard rings was considered as a possible contributor to the higher damage in the Perkin Elmer structure. Significant levels of carrier removal could change the doping profile of the lightly-doped multiplication region, causing decreases in APD breakdown voltage, or guard ring failure, which would cause runaway surface dark currents. Fig. 8 compares the dark I–V curves of a Perkin Elmer sample prior to irradiation and following irradiation to 2×10^{12} p/cm^2.

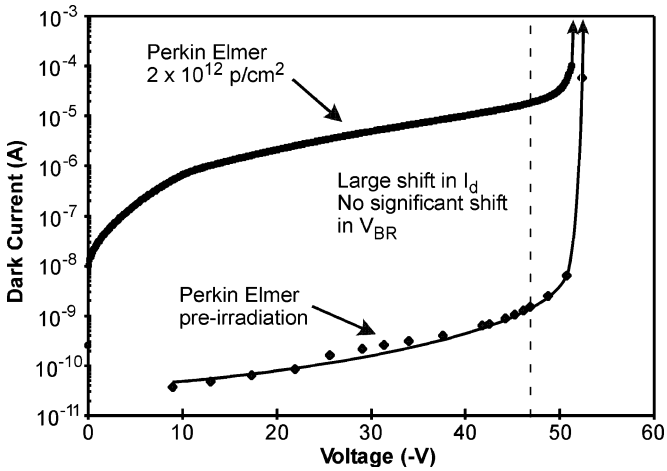

Fig. 8. Dark I–V profiles of a Perkin Elmer InGaAs APD prior to and following irradiation.

Although we see the same large increases in I_d at all bias conditions as we did at the operational voltage, there was not a significant shift in breakdown voltage following the highest radiation level used in this study. Also, if carrier removal was causing a guard ring failure, we would expect the resulting increase in dark current to be abrupt after a given fluence, not linear as observed. The stability of $V_{\rm BR}$ with irradiation also indicates that the APD gain is probably not being effected as we irradiate, dark current is just increasing very dramatically from the creation of carrier generation centers. Worth noting, APD $V_{\rm BR}$ is usually characterized as the voltage at which the dark current is a specified amount (10 μA for our InGaAs APDs). Radiation-induced increases in dark current beyond this level at the operational voltage do not imply that a shift in $V_{\rm BR}$ has occurred; full I–V characterization confirmed this for the Perkin Elmer device.

E. Possible Contributors to InGaAs Damage Factor Differences

There are several possible contributors to the larger damage factor in the Perkin Elmer APD.

1) Our results for Si APDs [5] showed that differences in doping appeared to contribute to differences in damage factors between structures. More highly doped depletion regions suffered higher dark current increases per unit volume, which may have been due to a higher likelihood of the creation of radiation-induced carrier generation centers in the devices with higher carrier concentration. Previous observations with Si have shown a tendency for damage coefficients to increase with carrier concentration [15]. The InGaAs absorption region of the Perkin Elmer APD may be more highly doped than the Hamamatsu APD and suffering more significant carrier generation and greater leakage current increases.
2) Although a small contributor to dark current increases in the Laird *et al.* study, it is possible that displacement damage in the InP multiplication region could have varying degrees of importance in our two InGaAs APDs. This would depend on the doping levels and volumes of the multiplication regions, and could be contributing to the differences in damage factors.
3) Some InGaAs APDs incorporate a highly doped InP charge layer between the multiplication and absorption regions. This supports a high enough field in the InP multiplication region for avalanche to occur and a low enough field in the InGaAs absorption region to mitigate tunneling effects [16]. The presence of such a layer could contribute to additional carrier generation issues, and this could be another reason why the Perkin Elmer damage factor is high. Furthermore, if the delicate balance between the n^+ InP charge layer density and the curvature of the guard doping profile is shifted from optimal, higher gains at the periphery ("edge") of the active volume, under the guard rings, can exceed that of the active area [13] (see Fig. 7), causing further multiplication of dark current. Carrier removal in the charge layer could tip the charge density away from optimal, causing higher dark current multiplication at the edge. It is also possible that a nonoptimal balance could exist prior to irradiation. Both situations could lead to a higher damage factor.

F. Selection Considerations

Large shifts in dark current from proton irradiation were observed in the InGaAs and Ge APDs in this study. This would be an important consideration when selecting a near infrared APD for a space based optical communications application where noise and BER are important, since increases in dark current decrease signal to noise ratio. An additional concern is that charge collection due to single event transients (SET) would be multiplied in an APD that is being utilized for high sensitivity and signal to noise ratio.

Although even the pre-irradiation dark current is high for the Ge APD (~300 nA at $M = 3$), relatively high dark current and noise does not prohibit the use of an APD. In application, it is undesirable for the noise of the system amplifier to exceed the detector noise. In light of this, Ge APDs can be used in applications where amplifier noise is relatively high, in environments with high electro-magnetic interference, for example [2]. Ge APDs can also be cooled to temperatures as low as 77 K to reduce dark current and noise, as is the case in photon-counting applications [17]. The order of magnitude increase in dark current by the highest fluence level is significant, although fractional dark current increases were much higher in the InGaAs APDs.

V. Conclusion

We have compared 63-MeV proton and Co-60 gamma radiation results for Ge and InGaAs APDs, suitable for applications at 1.3 and 1.55 μm. Dark current changes in these devices appear to be dominated by displacement damage in the bulk material. Dark current in these near infrared APDs was observed to increase by up to four orders of magnitude above pre-irradiation values by a 63-MeV proton fluence of 2×10^{12} p/cm^2. The magnitude of the dark current changes at typical operational gains were similar to prior results for silicon APDs, despite the smaller active areas and depletion regions of the APDs studied here (up to four orders of magnitude smaller). This similarity has been attributed to the differences in the material properties of Si, Ge, and InGaAs, and the relative radiation responses of these materials. We have also proposed that the structural complexity of InGaAs APDs makes it is difficult to predict their radiation response based on analysis of the volume or doping of the InGaAs absorption region alone. We caution that vulnerability to edge breakdown and nonuniform gain in the "edge" region for separate absorption-charge-multiplication (SACM) APDs have been identified by others. This could be a problem at very high fluences where carrier removal could exacerbate this design difficulty [13].

We note that the importance of dark current levels, before or after irradiation, depends entirely on the application and system noise requirements. Wide variations in APD device structure exist. For example, InGaAs APDs use an InP substrate, separate multiplication (InP) and absorption (InGaAs) regions, and an InGaAsP transition region to control charge buildup at the heterojunction interfaces. However, there are different InGaAs APD fabrication approaches, including mesa structures and planar structures with various styles of guard rings [11], [12], [17], [18]. Previous work [5] has shown that structural differences can have a large effect on the radiation responses of Si APD technologies, and bulk and surface damage can have varying degrees of dominance depending on structure.

Acknowledgment

The authors would like to acknowledge the technical assistance of T. F. Miyahira and B. G. Rax. They would also like to thank R. P. Ruiz for SEM and EDS analysis of the APD structures.

REFERENCES

[1] K. Shaik and K. Hemmati. (1995, Feb.) Wavelength Selection Criteria for Laser Communications. NASA Tech Report. [Online]. Available: http://techreports.jpl.nasa.gov/1995/95-0330.pdf, Jan. 2004

[2] P. P. Webb, R. J. McIntyre, and J. Conradi, "Properties of avalanche photodiodes," *RCA Rev.*, vol. 35, pp. 234–278, June 1974.

[3] G. S. Mecherle, Fundamentals of free space laser communication, in Jet Propulsion Laboratory Invited Lecture, Pasadena, CA, Sept. 17, 2003.

[4] W. N. Waggener, *Pulse Code Modulation Systems Design*. Norwood, MA: Artech House, 1999.

[5] H. N. Becker, T. F. Miyahira, and A. H. Johnston, "The influence of structural characteristics on the response of silicon avalanche photodiodes to proton irradiation," *IEEE Trans. Nucl. Sci.*, vol. 50, pp. 1974–1981, Dec. 2003.

[6] S. M. Sze, *Physics of Semiconductor Devices*, 2nd ed. New York: Wiley, 1981.

[7] J. R. Srour, C. J. Marshall, and P. W. Marshall, "Review of displacement damage effects in silicon devices," *IEEE Trans. Nucl. Sci.*, vol. 50, pp. 653–670, June 2003.

[8] P. W. Marshall, C. J. Dale, G. P. Summers, and E. A. Wolicki, "Proton, neutron, and electron-induced displacement damage in germanium," *IEEE Trans. Nucl. Sci.*, vol. 36, pp. 1882–1888, Dec. 1989.

[9] G. P. Summers, E. A. Burke, P. Shapiro, S. R. Messenger, and R. J. Walters, "Damage correlations in semiconductors exposed to gamma, electron and proton radiations," *IEEE Trans. Nucl. Sci.*, vol. 40, pp. 1372–1379, Dec. 1993.

[10] J. R. Srour, S. C. Chen, S. Othmer, and R. A. Hartmann, "Radiation damage coefficients for silicon depletion regions," *IEEE Trans. Nucl. Sci.*, vol. 26, pp. 4784–4791, Dec. 1979.

[11] Y. Liu, S. R. Forrest, J. Hladky, M. J. Lange, G. H. Olsen, and D. E. Ackley, "A planar InP/InGaAs avalanche photodiode with floating guard ring and double diffused junction," *J. Lightwave Technol.*, vol. 10, pp. 182–193, Feb. 1992.

[12] K. Taguchi, T. Korikai, Y. Sugimoto, K. Makita, and H. Ishihara, "Planar-structure InP/InGaAsP/InGaAs avalanche photodiodes with preferential lateral extended guard ring for 1.0–1.6 um wavelength optical communication use," *J. Lightwave Technol.*, vol. 6, pp. 1643–1655, Nov. 1988.

[13] J. S. Laird, T. Hirao, S. Onoda, H. Ohyama, and T. Kamiya, "Heavy-ion induced single-event transients in high-speed InP-InGaAs avalanche photodiodes," *IEEE Trans. Nucl. Sci.*, vol. 50, pp. 2225–2232, Dec. 2003.

[14] S. Kuboyama, H. Sindou, T. Hirao, and S. Matsuda, "Consistency of bulk damage factor and NIEL for electrons, protons, and heavy ions in Si CCDs," *IEEE Trans. Nucl. Sci.*, vol. 49, pp. 2684–2689, Dec. 2002.

[15] J. R. Srour, S. Othmer, and K. Y. Chiu, "Electron and proton damage coefficients in low-resistivity silicon," *IEEE Trans. Nucl. Sci.*, vol. NS-22, pp. 2656–2662, Dec. 1975.

[16] K. K. Loi and M. Itzler, "Avalanche photodetectors for 10 Gb/s fiber optic receivers," *Compound Semicond.*, vol. 6, no. 3, pp. 1–3, April 2000.

[17] A. Lacaita, F. Zappa, S. Cova, and P. Lovati, "Single-photon detection beyond 1 μm: performance of commercially available InGaAs/InP detectors," *Appl. Opt.*, vol. 35, no. 1, pp. 2986–2996, June 1996.

[18] J. C. Campbell, B. C. Johnson, G. J. Qua, and W. T. Tsang, "Frequency response of InP/InGaAsP/InGaAs avalanche photodiodes," *J. Lightwave Technol.*, vol. 7, pp. 778–784, May 1989.